Altering the Onset of Cocontinuity in Nanocomposite Immiscible Blends by Acting on the Melt-Compounding Procedure

G. Filippone, D. Acierno

Dipartimento di Ingegneria dei Materiali e della Produzione (Consorzio INSTM - UdR Napoli), Università di Napoli "Federico II," Piazzale Tecchio, 80, 80125, Napoli, Italy

Received 28 April 2011; accepted 28 April 2011
DOI 10.1002/app.34785
Published online 11 August 2011 in Wiley Online Library (wileyonlinelibrary.com).

ABSTRACT: The addition of nanoparticles to polymer systems with an existing phase-separated morphology, such as polymer blends, represents an innovative approach to controlling the microstructure and, hence, the macroscopic properties of the material. During the melt mixing of the constituents, the particles migrate toward specific regions of the material and are driven by more favorable thermodynamic interactions. Kinetic effects related to the high viscosity of the polymer melts, however, may lead to nonequilibrium morphologies. This makes the mixing procedure crucial for controlling the space distribution of the filler and, hence, the microstructure of the blend and its final properties. We focused on this topic by investigating the effect of the sequence of addition of the constituents in blends of polystyrene and polyamide 6 filled with an organoclay prepared by melt compounding. We show that the mixing procedure could bring about alterations in the onset of cocontinuity, which could be exploited to enhance the high-temperature mechanical strength of the blends. © 2011 Wiley Periodicals, Inc. J Appl Polym Sci 122: 3712–3719, 2011

Key words: blends; immiscibility; melt; nanocomposites; structure–property relations

INTRODUCTION

A considerable portion of the market of plastic materials is dominated by a limited number of commodity polymers. Nevertheless, the increasing demand of materials for advanced applications or characterized by specific combinations of properties cannot be satisfied by simple homopolymers. This explains the remarkable technological and scientific interest in the modification or mixing of these commodity polymers, with the aim of attaining performances that are currently exhibited solely by expensive engineering resins or nonpolymeric materials. In the last 20 years, it has been widely demonstrated that the addition of nanosized particles can lead to surprisingly high performances, even for very low filler amounts.[1] Although there are many examples of nanofilled polymers with excellent mechanical, optical, thermal, and transport properties, limiting the capability offered by the use of nanoparticles to the mere capitalization of the filler properties appears nowadays restrictive. Instead, a genuine nanocomposite should exhibit new behavior and properties that are totally absent in the unfilled matrices. In line with this aim, one of the last challenges in the field of nanocomposites foresees the use of nanoparticles as a medium to drive the formation of desired nanostructures and microstructures in multiphase polymeric materials.[2] The addition of nanoparticles to a block copolymer has recently been revealed as an elegant way to control the spatial distribution and orientation of the filler; this has given new perspective to the understanding of the physics of self-assembling and to many technological applications.[3] Similarly, small amounts of nanometric particles have been revealed to be able to radically affect the microstructure of immiscible polymer blends, either by causing a drastic reduction of the characteristic size of the minor phase[4–8] or by promoting the unexpected formation of cocontinuous morphologies.[9–16] The latter topic is, today, a matter of intensive investigation because of the remarkable combination of functional and structural properties generally exhibited by cocontinuous blends.[17–19] Recent results have shown that the uneven distribution of the filler and, in particular, its gathering at the interface play a major role in the alteration of the onset of cocontinuity.[16] The balance of mutual interactions among particles and liquid phases represents the first-order parameter governing the final distribution of the filler inside low-viscosity emulsions.[20] In contrast, when two polymers are

Correspondence to: G. Filippone (giovanni.filippone@unina.it).

Contract grant sponsor: Italian Ministry of University and Research; contract grant number: PRIN 2007 protocol number 20077R3PXF.

blended with a nanometric filler, the equilibrium is not immediately attained because of the high viscosity of the suspending medium; this makes crucial processing parameters, such as the mixing procedure.[21] Specifically, the order of addition of the components can have a strong effect because it has a direct influence on the medium with which the filler will be in contact during the course of its incorporation.[22] This topic was addressed in this study, where an organomodified montmorillonite was added to blends of polystyrene (PS) and polyamide 6 (PA6) at different compositions with two different compounding procedures. Specifically, we focused on the relevance of the order of addition of the constituents to the final blend microstructure, with special emphasis on the ability of nanoparticles to alter the onset of phase cocontinuity. Wide-angle X-ray diffraction (WAXD), transmission electron microscopy (TEM), scanning electron microscopy (SEM), and extraction tests with selective solvents were performed to investigate the structure of the materials at both the nanoscale and the microscale. The morphological features of the blends were related to their high-temperature mechanical behavior, which was investigated through dynamic mechanical analysis (DMA).

EXPERIMENTAL

Materials

The polymeric constituents of the blends were atactic PS [kindly supplied by Polimeri Europa (Mantova, Italy), weight-average molecular weight = 268 KDa, zero-shear rate viscosity = $2.26 \cdot 10^4$ Pa s at temperature (T) = 200°C; glass-transition temperature (T_g) ≈ 100°C] and PA6 [Radilon S from Radici Group, Bergamo, Italy, $\rho = 1.13$ g/cm^3, melting temperature (T_m) ≈ 210–220°C]. As a filler, we used a montmorillonite modified with dimethyl dihydrogenated tallow quaternary ammonium cation (Cloisite 15A from Southern Clay Products, Gonzales, TX; concentration of the organomodifier = 125 mequiv/100 g of clay, $\rho = 1.66$ g/cm^3).

We prepared the blends by melt-compounding the constituents using a corotating twin-screw extruder suitable for distributive mixing (Minilab Microcompounder by Thermo Fischer Scientific Inc.) equipped with a cylindrical capillary die (diameter = 1.5 mm, length = 10 mm). The extrusions were performed at T = 240°C, and the screw speed was set to 100 rpm; this corresponded to average shear rate of about 50 s^{-1}. The processing time, set to about 300 s for all the samples, was accurately controlled by means of an integrated backflow channel. The extrusion chamber was saturated with gaseous nitrogen to minimize thermooxidative degradation phenomena during the process.

Blends at different compositions were prepared with two different compounding procedures. In the first one, indicated in the following as "two-step procedure," the filler and the polymers were loaded simultaneously into the extruder. In the second procedure, indicated as "two-step procedure," the filler was incorporated inside the PA6 in a first extrusion step, and then, the resulting homopolymer nanocomposite was melt-compounded with the PS through a second extrusion. In the single-step procedure, the PA6 was previously extruded under the same conditions of the other samples to ensure that all of the polymeric fractions of the blends had experienced the same thermomechanical history. We varied the filler content by keeping constant the weight ratio between PA6 and clay to a value of clay/PA6 = 0.05. The compositions of the blends are summarized in Table I. The extrudate was compression-molded for 3 min at T = 250°C and pressure ≈ 100 bar with a laboratory press (LP-20B by Lab Tech Eng Co., Ltd., Samut Prakan, Thailand). The subsequent characterizations were all performed on the resulting disks (diameter = 25 mm, thickness ≈ 1.5 mm).

TABLE I
Compositions and Designations of the Samples

Sample	Composition [w/w (+ pphr)]	Designation
PS/PA6	50/50	50PS
PS/PA6	60/40	60PS
PS/PA6	70/30	70PS
PS/PA6	80/20	80PS
PS/PA6 + Cloisite 15A	50/50 + 2.5	50PS + clay
PS/PA6 + Cloisite 15A	60/40 + 2	60PS + clay
PS/PA6 + Cloisite 15A	70/30 + 1.5	70PS + clay
PS/PA6 + Cloisite 15A	80/20 + 1	80PS + clay
PS/PA6 + Cloisite 15A	90/10 + 0.5	90PS + clay

Characterization techniques

A stress-controlled rotational rheometer (model ARG2 by TA Instruments, New Castle, DE) in parallel-plate geometry (plate diameter = 25 mm) was used for the rheological experiments. Steady-state shear experiments were carried out at T = 240°C in a dry nitrogen atmosphere.

The degree of continuity of the PA6 phase (ϕ_{PA6}) was estimated through quantitative extraction experiments. Sample having an initial mass M_0 were immersed at room temperature into a beaker containing 200 mL of reagent-grade formic acid, a selective solvent for PA6, and gently stirred for about 48 h. Then, the sample was carefully dried in a vacuum oven and weighed again. The procedure was repeated until a constant mass M_f was attained; this typically required three reiterations. All of the samples remained self-supporting at the end of the experiments. The values of ϕ_{PA6} were evaluated as the ratio between the mass of PA6 removed during extraction (m^{lost}_{PA6}) and the mass initially present in the sample (m^0_{PA6}): $\phi_{PA6} = m^{lost}_{PA6}/m^0_{PA6}$. In unfilled blends,

TABLE II
σ^d and σ^p Components of the Surface Tensions and Temperature Coefficients ($d\sigma/dT$) of the Blend Constituents and Wetting Parameter of PA6 (ω_{PA6}) at T = 240°C

Material	T (°C)	σ^d (mN/m)	σ^p (mN/m)	$d\sigma/dT$ (mN/m K)	ω_{PA6}
PS	20	34.5[a]	6.1[a]	−0.072[a]	
PA6	260	21.6[b]	9.3[b]	Not applicable	
Cloisite 15A	20	43.3[c]	14.4[c]	−0.13[c]	−0.24[d]

[a] Data from ref. 26.
[b] Data from ref. 27.
[c] Typical data for organo clay taken from ref. 28.
[d] Estimated assuming σ_{PA6} at 240°C ≈ to σ_{PA6} at 260°C.

m_{PA6}^{lost} was simply given by the recorded weight loss $\Delta M = M_0 - M_f$, whereas $m_{PA6}^{lost} = M_0 - M_f = \Delta M$, whereas for the filled samples, an unknown fraction of particles was lost together with the removed PA6. In this case, only a range of possible ϕ_{PA6}'s could be evaluated. The upper limit of this range referred to the case in which only the polymer was removed so that $m_{PA6}^{lost} = \Delta M$. The lower limit was computed with the consideration that at worst, the filler entirely located inside the PA6 and it was totally lost during extraction, that is, $m_{clay} = \Delta M - m_{clay}^{lost} = \Delta M - 0.05 * m_{PA6}^{lost} = \Delta M/1.05$, where m_{clay} is the total mass of filler in the sample.

Wide-angle X-ray analyses were performed at room temperature in the reflection mode on an X-ray diffractometer (D-500 by Siemens AG, Munich, Germany) with Cu Kα radiation with a wavelength of 1.54 Å, with a scanning rate of 10°/min. The interlayer spacing between the silicate layers of the organoclay (d_{001}) was computed by the application of Bragg's law to the low-angle peak ($2° < 2\theta < 4°$) of the scattering intensity.

TEM was used to inspect the state of dispersion of the filler with a TEM (EM 208 by Philips, Amsterdam, the Netherlands) with a 100-keV accelerating voltage. The observations were carried out on thin slices (thickness < 100 nm) microtomed at room temperature with a diamond knife.

The microstructure of the blends was examined with a scanning electron microscope (SEM Phenom by FEI, Hillsboro, OR). The inspected cryofractured surfaces of the samples were previously coated with chromium.

The DMA was carried out with a Tritec 2000 DMA apparatus (Triton Technology Ltd., Grantham, UK). The moduli were measured as a function of temperature in single-cantilever bending mode at a frequency (ω) of 1 Hz and a total displacement of 0.05 mm, which was small enough to be in the linear regime. The sample bars (size ≈ 8 × 20 × 1.5 mm^3) were heated at 2°C/min from room temperature.

RESULTS AND DISCUSSION

Preliminary considerations

When solid particles are added to a mixture of immiscible fluids, the filler typically distributes unevenly as a consequence of its different affinities with the two liquids. In principle, the Flory–Huggins interaction parameters can be used to predict which of two polymers has a higher affinity with the filler.[23] When one deals with organomodified clay, however, several assumptions are required about the contribution of the organic surfactant, which may bring about some uncertainty in the calculations. Alternatively, the localization of a filler (subscript *f*) in a blend constituted by the polymers (subscripts *A* and *B*) at thermodynamic equilibrium can be predicted through the wetting parameter of *A* (ω_A), defined as follows:[24]

$$\omega_A = \frac{\sigma_{f-B} - \sigma_{f-A}}{\sigma_{A-B}} \quad (1)$$

where σ_{i-j} is the interfacial energy, which can be calculated with the Owens–Wendt equation:

$$\sigma_{i-j} = \sigma_i + \sigma_j - 2\left(\sqrt{\sigma_i^d \sigma_j^d} + \sqrt{\sigma_i^p \sigma_j^p}\right)$$

where σ^d and σ^p are the dispersive and specific parts of the surface energy, respectively: $\sigma = \sigma^d + \sigma^p$.[25] If $\omega_A > 1$ ($\omega_A < 1$), the filler enriches phase A (phase B), whereas for $|\omega_A| < 1$, it accumulates at the interface.

The wetting coefficients for our systems, shown in Table II, were obtained from literature values of the surface energies extrapolated at the processing temperature with the assumption of a linear dependence of σ on T.[26–28] The computed value of ω_{PA6} indicates that at thermodynamic equilibrium, the filler locates at the interface. In mixtures of high-viscosity fluids, such as polymer melts, however, the kinetic effects play a crucial role, and the blend may be frozen in a nonequilibrium morphology; this strongly depends on the conditions of the mixing process. The effect of the compounding procedure on the blend morphology is discussed in the following paragraph, with special emphasis on the impact of the phase-inversion composition (Φ_I).

Morphological analyses

The final microstructure of unfilled blends is the result of a dynamic interplay among breakup,

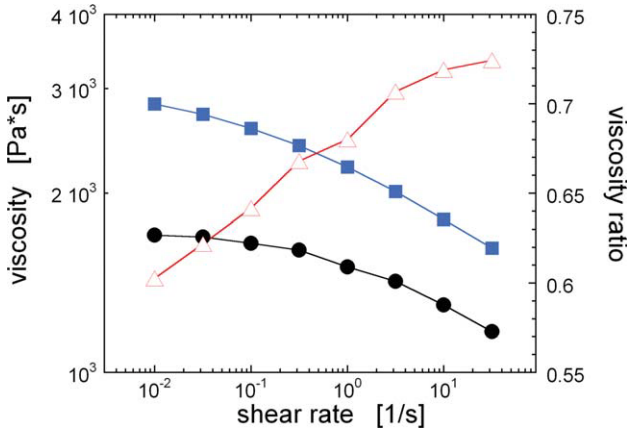

Figure 1 Left axis: shear viscosity of (■) PS, (●) PA6, and PA6 filled with Cloisite 15A (clay/PA6 weight ratio = 0.05). Right axis: (△) viscosity ratio of the unfilled blend: $p(\dot{\gamma}) = \eta_{PA6}/\eta_{PS}$. [Color figure can be viewed in the online issue, which is available at wileyonlinelibrary.com.]

coalescence, and relaxation phenomena occurring during flow and also at rest.[29] For low amounts of either of the phases, immiscibility results in droplet–matrix morphologies. Increasing the content of the dispersed phase eventually leads to phase inversion. At Φ_I, the distinction between the disperse and matrix phases vanishes, and both phases result continuous.[30] Actually, in unfilled polymer blends, cocontinuity occurs in a quite large range of compositions around Φ_I. Several semi-empirical models and theories exist relating Φ_I to the ratio between the viscosities of the blend constituents (p).[31–33] The steady-state shear viscosities of the neat polymers at $T = 240°C$ are shown in Figure 1 as a function of the shear rate ($\dot{\gamma}$), together with the ratio between the shear viscosity (η) of PA6 and PS:

$$p(\dot{\gamma}) = \eta_{PA6}/\eta_{PS}$$

The predictions of the models, carried out at $\dot{\gamma} \approx 30\ s^{-1}$, that is, close to the conditions experienced by the materials during the extrusions, are summarized in Table III for our unfilled PS/PA6 blend and give values for the phase inversion composition of PA6 ($\Phi_{I\text{-PA6}}$) ranging between 0.4 and 0.5. Such an approach could not be used for the filled systems. In these more complex systems, in fact, rheological models merely based on the viscosity ratio are well-known to fail in the prediction of Φ_I.[9,13]

The results of quantitative extraction experiments are shown in Figure 2. We observe that this kind of analysis systematically overestimates the degree of continuity of the soluble phase of samples with a globular morphology because of the removal of the droplets located in a thin surface layer.[34] Focusing

TABLE III
Predictions of the Phase Inversion Composition for the Unfilled Blend Based on Different Rheological Models

Model	Equation	$\Phi_{I\text{-PA6}}$ (%)[a]
Miles and Zurek[32]	$\frac{\Phi_{I-1}}{\Phi_{I-2}} = \frac{\eta_1(\dot{\gamma})}{\eta_2(\dot{\gamma})}$	0.43
Utracki[33]	$\Phi_{I-2} = \frac{1}{2}\left(1 - \frac{\log(\eta_1/\eta_2)}{[\eta]}\right)$	0.48
Everaet et al.[34]	$\frac{\Phi_{I-1}}{\Phi_{I-2}} = \left(\frac{\eta_1(\dot{\gamma})}{\eta_2(\dot{\gamma})}\right)^{0.3}$	0.52

[a] Values computed at $\dot{\gamma} = 30\ s^{-1}$.

on the samples with high extent of PA6 phase continuity ($\varphi_{PA6} \sim 0.9$), however, it is clear that the presence of the filler results in a reduction of the critical content for the PA6 phase continuity with respect to the unfilled system. Interestingly, such effect is more pronounced for the samples prepared via the single-step procedure. To explain such a result, we have to consider all the phenomena occurring since the earlier stages of the mixing process.

In the single-step procedure, a mixture of solid polymer pellets, particles, and a viscous fluid mainly constituted by the polymer having the lower T_m/T_g initially formed soon after the constituents were loaded inside the extruder. At this stage, the particles could be incorporated by the molten polymer, regardless of wettability considerations. Because the PS softens at a temperature lower than the melting of the PA6, it is possible that in our samples, the filler could have remained initially embedded inside the PS. In contrast, in the two-step procedure, the filler originally resides inside the PA6. In both cases, different scenarios are possible, where the filler may

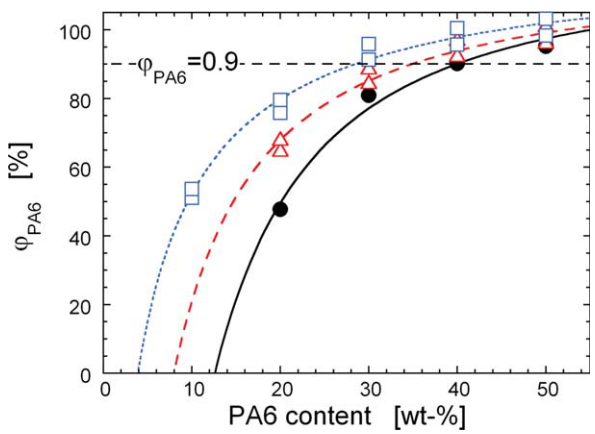

Figure 2 Extent of continuity of the PA6 phase as a function of the PA6 content for the (●) unfilled and filled blends prepared with the (□) single-step and (△) two-step procedures; the pairs of points shown for each composition for the two nanocomposite systems represent the lower and upper limits of possible ϕ_{PA6} estimated as described in the Experimental section. The interpolating lines are sigmoidal fits to the experimental points. [Color figure can be viewed in the online issue, which is available at wileyonlinelibrary.com.]

TABLE IV
Interlayer Spacing Between the Silicate Platelets of the Organoclay for the Pristine Filler and the 50PS + Clay Samples Prepared by Means of the Two Mixing Procedures

Sample	2θ (°)	d_{001} (nm)
Cloisite 15A	2.81	3.14
50PS + clay (single-step)	2.62	3.37
50PS + clay (two-step)	2.59	3.41

or may not have the opportunity to migrate toward the interface driven by thermodynamics within the processing times. During their motion, the particles affect the microstructural evolution of the polymer melts, and the structural evolution of the fluids, in turn, affects the dispersion of the particles.[35] Therefore, the final microstructure of the filled samples depends on the complex interplay among the phase-separation phenomena and wetting. This made the prediction of the final morphology very difficult and made targeted morphological analyses indispensable for assessing the actual distribution of the filler inside the blends.

The results of WAXD are summarized in Table IV in terms of interlayer spacing between the silicate platelets. Measurements were carried out on the pristine filler and the 50PS + clay samples prepared through the two melt-mixing procedures. The two blends exhibited a comparable, slight increase of d_{001} with respect to the neat organoclay; this means that a small intercalation of polymer chains between the silicate layers occurred during the melt mixing, regardless of the compounding procedure. Nothing could be said about the presence of exfoliated platelets, which were not detectable through WAXD.

TEM analyses were performed to get a direct visualization of the filler inside the composites. The micrographs of the single-step 90PS + clay and two-step 80PS + clay blends are shown in Figure 3.

The PA6 phase is in the form of droplets a few micrometers in size. The magnifications of such inclusions reveal that a detachment between the phases at the polymer–polymer interface occurred during the cutting of the samples. It was clear, however, that most of the particles reside inside the PA6 phase, regardless of the mixing procedure. The disagreement with the wettability calculations may have originated from many factors. Among others, we observe that degradation of the organomodifier of the filler was likely to occur at the processing temperature.[36] This may have enhanced the polar features of the particles and made them more affine with the polyamide. Focusing on the edge of the PA6 droplets, however, well-aligned exfoliated platelets and/or few-layer stacks were noticed at the interface. Such an occurrence was more frequently observed for the blends prepared via the single-step procedure. This could be related to the differences noticed between the two families of samples in terms of Φ_I. Specifically, in line with recently published results, the platelets located at the interface may have resulted more efficient in shifting of the onset of cocontinuity because of the noticeable alterations of the interface rheology.[16]

SEM observations were performed to investigate the micrometer-scale arrangement of the polymer phases in the blends. The micrographs reported in Figure 4 show the fracture surfaces of the unfilled and filled blends at 20 and 50 wt % PA6. The samples were etched with formic acid to remove the polyamide phase; this enhanced the contrast.

The unfilled 80PS sample exhibits the typical globular morphology of immiscible blends far from cocontinuity, with spherical PA6 droplets with an average diameter (D_N) of

$$D_N = \sum_{i=1}^{N} d_i/N = 4.8\mu\text{m}$$

as obtained by analysis of the sizes (d_i) of $N \approx 300$ droplets [Fig. 4(a)]. A coarse interpenetrated microstructure characterizes the highly cocontinuous 50PS

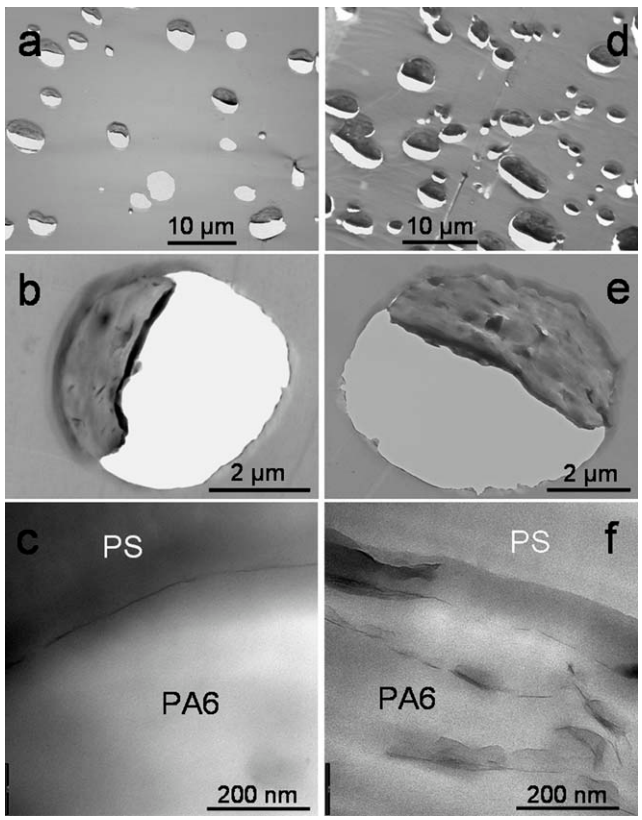

Figure 3 TEM micrographs of the (a–c) 90PS + clay samples prepared via the single-step procedure and (d–f) 80PS + clay samples prepared via the two-step procedure.

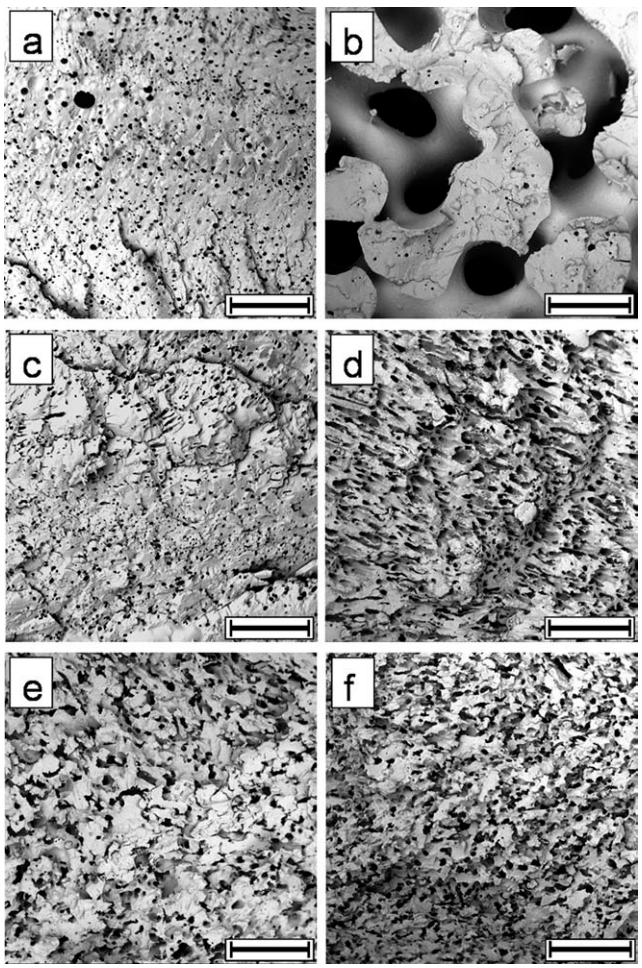

Figure 4 SEM micrographs of different samples: (a) 80PS, (b) 50PS, (c) 80PS + clay prepared via the two-step procedure, (d) 50PS + clay prepared via the two-step procedure, (e) 80PS + clay prepared via the single-step procedure, and (f) 50PS + clay prepared via the single-step procedure. The surfaces were etched with formic acid to remove the PA6 phase. The scale bars represent 100 μm.

sample [Fig. 4(b)]. The presence of isolated PA6 droplets trapped inside the structure of PS was noticed. These domains cannot be removed during extraction experiments, which explains the values of ϕ_{PA6} lower than 100% found even for the fully cocontinuous samples. The addition of the filler through the two-step procedure mainly caused a slight reduction of the characteristic size of the PA6 droplets in the sample at 20 wt % PA6 [Fig. 4(c)], which decreased to $D_N = 4.0$ μm. The presence of some elongated PA6 domains was observed; these suggested an incipient interconnection of the minor phase. This is in line with the results of the extraction experiments, which showed that this sample was close to the onset of cocontinuity. The impact of the filler was much more evident in the sample at 50 wt % PA6, where a clear refinement of the morphology was noticed [Fig. 4(d)]. The high value of ϕ_{PA6} measured for the sample at 20 wt % PA6 prepared via single-step procedure was supported by the corresponding SEM micrograph, which shows a highly cocontinuous microstructure [Fig. 4(e)]. The differences between the blends prepared with the two compounding procedures, however, seems reducing at high PA6 contents; the samples at 50 wt % PA6 share a comparable, finely interpenetrated morphology.

DMA

The morphological features of the samples clearly emerges when they were tested in dynamic conditions. The results of DMA analyses are reported in Figure 5, where the storage moduli (E''s) and loss factors (tan $\delta = E''/E'$, E'' being the loss modulus) are shown as a function of temperature for the neat polymers and the unfilled blends at different compositions.

The moduli of the pure polymers drop down at the respective T values, that is, at about 100°C for PS and about 65°C for PA6. However, whereas PS completely loses its mechanical strength above T_g, polyamide exhibits a plateau modulus up to the onset of melting ($T_m \approx 220$°C) because of its semicrystalline nature. The behavior of the unfilled blends reflects their microstructure: the PS matrix governs the response in the samples with a globular morphology (80PS and 70PS), whereas the PA6 continuous network ensures a finite plateau modulus above T_g of PS in the highly cocontinuous samples (60PS and 50PS). Obviously, the higher the PA6 content is, the more efficient the polyamide framework is in bearing stresses and, as a consequence, the higher the high-temperature plateau modulus is.

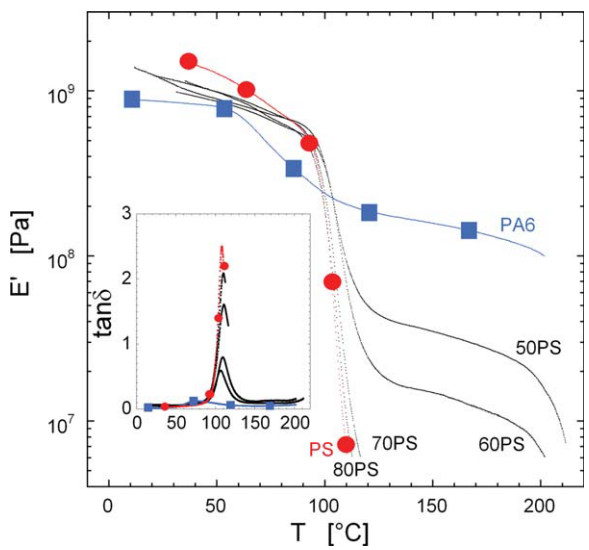

Figure 5 Temperature dependence of E' at $\omega = 1$ Hz for (●) PS and (■) PA6 and blends at different compositions. The inset shows the tan δ versus T. [Color figure can be viewed in the online issue, which is available at wileyonlinelibrary.com.]

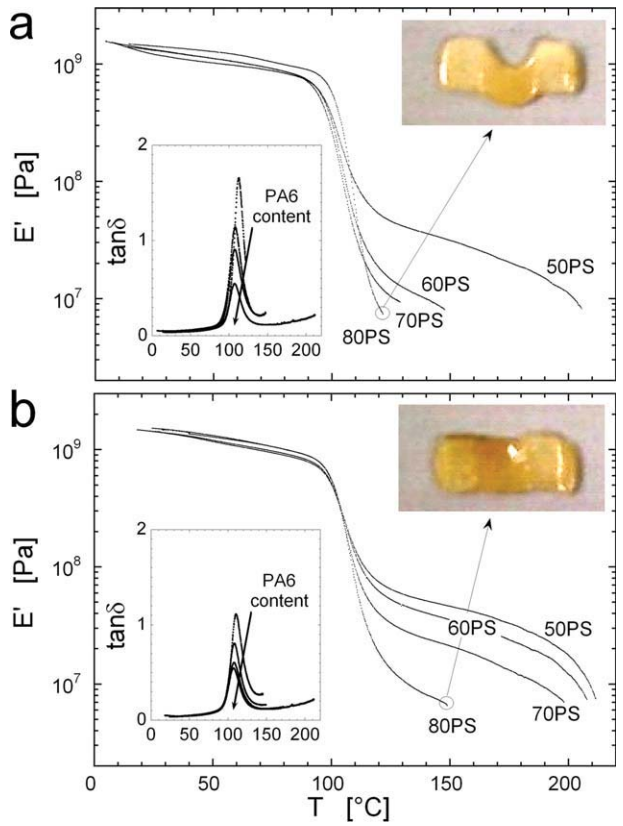

Figure 6 Temperature dependence of E' at $\omega = 1$ Hz for the filled blends at different compositions prepared via the (a) two-step and (b) single-step procedures. The tan δ versus T plots are reported in the insets. The pictures show the samples at 20 wt % PA6 at the end of DMA. [Color figure can be viewed in the online issue, which is available at wileyonlinelibrary.com.]

The addition of the filler is expected to have a double effect: on the one hand, the well-known reinforcing action of the particles should have enhance the overall mechanical properties of the blends; on the other hand, the filler affects the blend microstructure, which in turn, influences the macroscopic response of the samples. The results of DMA are shown in Figure 6 for the filled blends prepared with the two compounding procedures.

Each sample exhibits an enhanced glassy modulus with respect to its unfilled counterpart. The mixing procedure, however, did not have a noticeable effect below the glass transition of the polymers. At higher temperatures, the PS softens, and the mechanical response of the blends depends on the degree of structuring of the PA6 phase. In these conditions, the microstructural differences between the two families of samples clearly emerge. As for the unfilled blends and regardless of the compounding procedure, the higher the PA6 content is, the higher the residual modulus is and the wider the temperature range in which it could be appreciated is. The single-step compounding procedure, however, was more effective in anticipating the onset of the PA6 phase continuity. As a result, the samples prepared in this way exhibit a higher degree of cocontinuity, and hence, higher moduli of the corresponding blends obtained via the two-step procedure. The difference between the two compounding techniques is evident, especially at low amounts of PA6. The sample at 20 wt % PA6 prepared through the single-step procedure exhibits an appreciable plateau modulus above T_g of PS because of its high extent of PA6 phase continuity, so differentiating itself from the sample at the same composition prepared in two steps. As shown in Figure 6, this apparently slight difference has a remarkable consequence on the macroscopic behavior of the materials: the single-step sample keeps its structural integrity, even at high temperatures, whereas the one prepared in two steps starts dripping between the clamps of the DMA apparatus when T_g of the PS matrix phase is exceeded.

Finally, a comparison between Figures 4(e) and 4(f) shows that in samples sharing a comparably high extent of PA6 phase continuity, the higher the polyamide content is, the finer and more branched the PA6 network is. This results in a gradual increase of the residual modulus above T_g of the PS, which probably benefits also from the better efficiency of the finely interpenetrated microstructures in bearing external stresses with respect to coarse morphologies, such those of the unfilled systems.[37]

CONCLUSIONS

Blends of PS and PA6 filled with organoclay were prepared by melt compounding. The sequence of addition of the constituents was varied to investigate the effect of the sequence of addition of the constituents on the microstructure and properties of the materials. In the single-step procedure, the filler and the polymers were loaded simultaneously into the mixing apparatus, whereas in the two-step procedure, a homopolymer-based PA6 nanocomposite was first prepared, and then, it was mixed with the PS. Morphological analyses showed that the filler mainly enriched the more polar PA6 phase, regardless of the mixing procedure. A fraction of particles, however, gathered at the polymer–polymer interface, as predicted on the basis of wettability considerations. This resulted in a general refinement of the blend morphology, regardless of the mixing procedure, which instead influenced Φ_I. Specifically, a more relevant reduction of the critical content of PA6 for cocontinuity was noticed in the system prepared via the single-step procedure with respect to the unfilled blend. The macroscopic mechanical properties of the samples reflected their microstructural features: the blends with a droplet–matrix

morphology behaved similarly to the major PS phase, whereas the PA6 phase contributed to the mechanical strength, even above the softening temperature of the PS in the blends with a high extent of phase cocontinuity. The presence of the filler added via the single-step procedure widened the range of cocontinuity and, thus, enhanced the mechanical strength at high temperatures because of the continuity of the PA6 phase. This allowed the preservation of the structural integrity of the samples, even in blends at low contents of polyamide.

Our results confirm the relevance of kinetic effects in nanofilled polymer blends and demonstrate that the compounding procedure represents a versatile parameter for the control of the morphology in complex multiphase systems, such as nanocomposite polymer blends.

The authors thank Pio Iannelli, University of Salerno, for the WAXD analyses and Naomi Lunadei and Gianfredo Romano for support in the experimental activity.

References

1. Jordan, J.; Jacob, K. I.; Tannenbaum, R.; Sharaf, M. A.; Jasiuk, I. Mater Sci Eng A 2005, 393, 1.
2. Manias, E. Nat Mater 2007, 6, 9.
3. Bockstaller, M. R.; Mickiewicz, R. A.; Thomas, E. L. Adv Mater 2005, 17, 1331.
4. Gelfer, M. Y.; Song, H. H.; Liu, L.; Hsiao, B. S.; Chu, B.; Rafailovich, M. J. Polym Sci Part B: Polym Phys 2003, 41, 44.
5. Khatua, B. B.; Lee, D. J.; Kim, H. Y.; Kim, J. K. Macromolecules 2004, 37, 2454.
6. Ray, S. S.; Pouliot, S.; Bousmina, M.; Utracki, L. A. Polymer 2004, 45, 8403.
7. Chow, W. S.; Mohd Ishak, Z. A.; Karger-Kocsis, J. Macromol Mater Eng 2005, 290, 122.
8. Hong, J. S.; Namkung, H.; Ahn, K. H.; Lee, S. J.; Kim, C. Polymer 2006, 47, 3967.
9. Li, Y.; Shimizu, H. Polymer 2004, 45, 7381.
10. Li, Y.; Shimizu, H. Macromol Rapid Commun 2005, 26, 710.
11. Wu, D.; Zhou, C.; Zhang, M. J Appl Polym Sci 2006, 1021, 3628.
12. Ray, S. S.; Bandyopadhyay, J.; Bousmina, M. Macromol Mater Eng 2007, 292, 729.
13. Zou, H.; Ning, N.; Su, R.; Zhang, Q.; Fu, Q. J Appl Polym Sci 2007, 106, 2238.
14. Filippone, G.; Dintcheva, N. T.; Acierno, D.; La Mantia, F. P. Polymer 2008, 49, 1312.
15. Filippone, G.; Dintcheva, N. T.; La Mantia, F. P.; Acierno, D. Polymer 2010, 51, 3956.
16. Filippone, G.; Romeo, G.; Acierno, D. Macromol Mater Eng 2011, 296, 658.
17. Pernot, H.; Baumert, M.; Court, F.; Leibler, L. Nat Mater 2002, 1, 54.
18. Pötschke, P.; Paul, D. R. Polym Rev 2003, 43, 87.
19. Dintcheva, N. T.; Filippone, G.; La Mantia, F. P.; Acierno, D. Polym Degrad Stab 2010, 95, 527.
20. Binks, B. P.; Horozov, T. S. Colloidal Particles at Liquid Interfaces; Cambridge University Press: Cambridge, England, 2006.
21. Fenouillot, F.; Cassagnau, P.; Majesté, J.-C. Polymer 2009, 50, 1333.
22. Elias, L.; Fenouillot, F.; Majesté, J.-C.; Martin, G.; Cassagnau, P. J Polym Sci Part B: Polym Phys 2008, 46, 1976.
23. Lim, S.-K.; Homg, E.-P.; Song, Y.-H.; Park, B. J.; Choi, H. J.; Chin, I.-J. Polym Eng Sci 2010, 50, 504.
24. Israelachvili, J. Intermolecular and Surface Forces; Academic: New York, 1992.
25. Owens, D. K.; Wendt, R. C. J Appl Polym Sci 1969, 13, 1741.
26. Solid Surface Energy Data (SFE) for Common Polymers. http://www.surfacetension.de/solid-surface-energy.htm (accessed July 2010).
27. As'habi, L.; Jafari, S. H.; Banghaei, B.; Khonakdar, A.; Pötschke, P.; Böhme, F. Polymer 2008, 49, 2119.
28. Picard, E.; Gauthier, H.; Gérard, J.-F.; Espuche, E. J Colloid Interface Sci 2007, 307, 364.
29. Filippone, G.; Netti, P. A.; Acierno, D. Polymer 2007, 48, 564.
30. Utracki, L. A. Commercial Polymer Blends; Chapman & Hall: London, 1998.
31. Miles, I. S.; Zurek, A. Polym Eng Sci 1988, 28, 796.
32. Utracki, L. A. Polym Mater Sci Eng 1991, 65, 50.
33. Everaet, V.; Aerts, L.; Groeninckx, G. Polymer 1999, 43, 6627.
34. Galloway, J. A.; Koester, K. J.; Paasch, B. J.; Macosko, C. W. Polymer 2004, 45, 423.
35. Peng, G.; Qui, F.; Ginzburg, V. V.; Jasnow, D.; Balazs, A. C. Science 2000, 288, 1802.
36. Scaffaro, M.; Mistretta, M. C.; La Mantia, F. P.; Frache, A. Appl Clay Sci 2009, 45, 185.
37. Filippone, G.; Dintcheva, N. T.; La Mantia, F. P.; Acierno, D. J Polym Sci Part B: Polym Phys 2010, 48, 600.